In-Well Pumping of a Membrane External-Cavity Surface-Emitting Laser

Davide Priante, Mingyang Zhang, Alexander R. Albrecht, Roman Bek, Michael Zimmer, Catherine L. Nguyen, David P. Follman, Garrett D. Cole, and Mansoor Sheik-Bahae

***Abstract*—We present a detailed characterization and comparative study of a membrane external-cavity surface-emitting laser (MECSEL) operating in the $\lambda = 1125$-1190 nm wavelength range under in-well pumping (at 1070 nm) and barrier-pumping (at 808 nm). The slope efficiency of the laser is significantly improved from 21% with barrier-pumping to 39% when pumping only the quantum wells at 1070 nm at a heat-sink temperature of 10 °C. To address the low pump absorbance with in-well pumping, we design and implement a low-aberration multi-pass pumping scheme. An optical output power of 28.5 W and slope efficiency of ∼28% is achieved with 8 circulating passes. This represents the highest output power demonstrated in any MECSEL, as well as the highest output power in-well pumped vertical external-cavity surface-emitting laser (VECSEL). It is noted that our reported output power is only limited by the available laser input power and no thermal roll-over is observed.**

***Index Terms*—In-well pumping, membrane external-cavity surface-emitting laser (MECSEL), optically-pumped semiconductor laser, sodium guide star lasers.**

I. Introduction

SINCE the first report of a vertical external-cavity surface-emitting laser (VECSEL) in 1997 [1] tremendous progress has been made in wavelength coverage, continuous-wave (CW) output power, and pulsed operation of these devices. Also referred to as semiconductor disk lasers (SDLs) or optically-pumped semiconductor lasers (OPSLs), these novel sources are of interest owing to their band gap engineering, high beam quality (M^2 near 1) and power scaling [2], [3], while benefitting from the advantages of the semiconductor gain characteristics [4].

Despite the above-mentioned advantages of VECSELs, the small gain volume renders them more susceptible to thermal degradation when pushing to high CW output powers, thus requiring innovative thermal management schemes.

In the typical "flip-chip" (bottom emitting) VECSEL design [5], heat is removed from the active region through the distributed Bragg reflector (DBR). Due to the small refractive index contrast of the constituent mirror materials, many layers are required to achieve sufficient reflectivity, resulting in a thick DBR with low thermal conductivity.

Moreover, the multiple interfaces scatter phonons, thus reducing the thermal diffusion, and increasing the thermal resistance. In fact, the thermal conductivity of the DBR is about one order of magnitude lower when compared to metallic mounting materials and heatsinks, and even lower compared to commonly used diamond heat spreaders.

Recently, a new OPSL platform has emerged, capable of mitigating the heat accumulation due to poor thermal conductivity of the integrated DBR in standard VECSELs. These so-called "DBR-free VECSELs" or membrane external-cavity surface-emitting-lasers (MECSELs) consist of the gain material only and thus bring attractive advantages for an OPSL architecture. In contrast to traditional VECSELs, MECSELs have a compact form factor and exhibit potentially superior thermal management [6]. Moreover, the lack of an epitaxial mirror opens up the possibility for emission at wavelengths at which a monolithic DBR may not be available due to restrictions imposed by lattice matching constraints. MECSELs comprise a semiconductor active region bonded to one [6] or sandwiched between two [7] high-thermal-conductivity heat spreaders (e.g., SiC or diamond). We employ two 10×10 mm² 4H-SiC heat spreaders in the double-side bonding approach to achieve better cooling efficiency and power scaling [6], [7]. Due to the absence of the monolithically integrated DBR, at least two external mirrors are utilized to form the laser cavity. The first demonstration of a MECSEL dates back to 2015 with a report of a maximum CW output power of 2.5 W and a 78 nm tuning range at 1160 nm [6]. Many other works followed with rapid progress in terms of output power and overall laser efficiency. In one example of relevant previous work, a comparison of single-side and double-side pumping was reported for a MECSEL emitting

Manuscript received April 8, 2021; revised July 11, 2021; accepted August 30, 2021. Date of publication September 2, 2021; date of current version October 1, 2021. This work was supported in part by the Air Force Research Laboratory under Contracts FA9451-17-P-0513 and FA9451-19-C-0504, in part by the UCSB Nanofabrication Facility, in part by the Center for Integrated Nanotechnologies (CINT), an Office of Science User Facility operated for the U.S. Department of Energy (DOE) Office of Science by Los Alamos National Laboratory (Contract DE-AC52-06NA25396), and in part by the Sandia National Laboratories (Contract DE-NA-0003525). The work of Davide Priante and Mansoor Sheik-Bahae was supported by the Air Force Office of Scientific Research under Contract FA9550-16-1-0362 (MURI). *(Corresponding author: Mansoor Sheik-Bahae.)*

Davide Priante, Mingyang Zhang, Alexander R. Albrecht, and Mansoor Sheik-Bahae are with the Department of Physics and Astronomy, University of New Mexico, Albuquerque, NM 87131 USA (e-mail: dpriante@unm.edu; myzhang@unm.edu; alex2@unm.edu; msb@unm.edu).

Roman Bek and Michael Zimmer are with the Twenty-One Semiconductors GmbH, 72654 Neckartenzlingen, Germany (e-mail: roman.bek@21semiconductors.com; michael.zimmer@21semiconductors.com).

Catherine L. Nguyen, David P. Follman, and Garrett D. Cole are with the Thorlabs Crystalline Solutions, Santa Barbara, CA 93101 USA (e-mail: cnguyen@thorlabs.com; dfollman@thorlabs.com; gcole@thorlabs.com).

Color versions of one or more figures in this article are available at https://doi.org/10.1109/JSTQE.2021.3109803.

Digital Object Identifier 10.1109/JSTQE.2021.3109803

at 780 nm. In that experiment, lasing threshold was reduced while the maximum output power as well as the slope efficiency were improved [8]. In the short-wavelength range, MECSELs emitting at a wavelength of 657 nm and 825 nm have been demonstrated showing power scaling capabilities and invariant M^2 with thermal lensing [7], [9]. Other works include an 80 nm tunable MECSEL, which constitutes the widest tuning range for this configuration, as well as reports covering devices with 10 and 16 W output powers with emission wavelengths near 1 μm respectively [10]–[12]. The longest wavelength demonstration was recently reported with a MECSEL emitting at 1770 nm and producing 3 W of output power at 20 °C [13]. The highest reported CW output power is 20 W at 1178 nm [14].

One of the main issues limiting the maximum output power in any OPSL structure is the parasitic heating induced by the large quantum defect (defined as the energy difference between the pump and emission wavelengths). In barrier pumped devices this amounts to more than 30% when using high energy photons as the excitation source. This large quantum defect can be circumvented when using the so-called "in-well" pumping scheme, where pump photons are absorbed by the quantum wells only. This allows for a significant reduction in the heat generated within the gain medium, which promises significant improvements in the overall laser power efficiency. Under these conditions, VECSELs with slope efficiencies in the range of 66-67% have been demonstrated [15]. While in-well pumping reduces the heat load in the active medium, it suffers from reduced pump absorption as a consequence of the short absorption length, given that the active region typically consists of less than ten quantum wells which may be a few nanometers each in thickness. To increase the pump absorption, multiple passes are required to achieve practical device performance. Such multi-pass pump configurations are standard in solid-state disk lasers, which utilize external pump optics allowing the pump light to recirculate several times. Traditional VECSEL devices have also reported the implementation of multi-pass pumping schemes [16]–[19].

The aim of this paper is to present a systematic comparison of in-well pumping and barrier pumping configuration in MECSELs. In the course of this work an output power of 28.5 W has been achieved using a multi-pass optical pumping scheme. Compared to barrier-pumped devices, our in-well pumped MECSEL shows an improvement in slope efficiency due to the significantly reduced quantum defect: 9.4% at 1070 nm compared to 31.4% when using an 808 nm pump. Another key result is the demonstration of a high-power MECSEL emitting around 1178 nm, which is a potential source for sodium guide star applications where the current technology is dominated by relatively complex laser sources. In this application space, MECSELs offer advantages in terms of low cost, high-efficiency, and compactness compared to established solid-state laser structures.

II. Gain Structure and Experimental Setup

Fig. 1(a) shows a schematic of the epitaxially grown MECSEL structure. It is fabricated by metal organic chemical vapor deposition (MOCVD) in a 3×2" showerhead reactor on a (100) GaAs substrate. The structural design is similar to that reported in [14], but with an increase in the number of quantum wells (QWs), 20 in this implementation. Due to the large number of QWs, this structure is optimized for in-well pumping (higher absorption per pass) and has a total thickness of 3.56 μm. The InGaAs quantum wells are embedded in GaAs barriers and arranged in a resonant periodic gain design [20]. 20 nm thick InGaP cladding layers prevent charge carrier recombination at the membrane surface and serve as protection for the substrate removal process. To balance the compressive strain introduced by the QWs, GaAsP strain compensation (SC) layers are used between the single QWs, resulting in a high-quality semiconductor surface which is suitable for direct bonding of the gain membrane to silicon carbide heat spreaders. A 250-nm-thick $Al_{0.92}Ga_{0.08}As$ etch stop layer is deposited below the membrane and later removed together with the substrate.

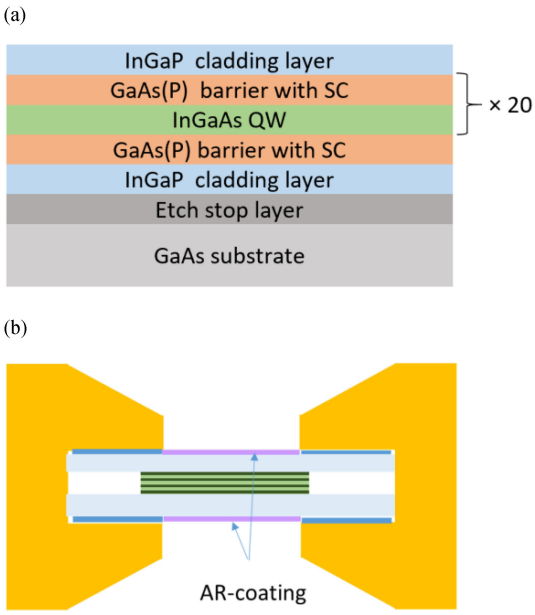

Fig. 1. (a) Schematic of the MOCVD-grown epi structure of the InGaAs-GaAs MECSEL with 20 QWs. (b) Sandwich-bonded semiconductor membrane (after substrate removal) between two AR-coated SiC substrates and two copper heatsinks. Indium foil is depicted in blue and the SiO_2 AR-coating is depicted in violet.

In our MECSEL, the gain membrane is sandwiched between two polished and low absorption single-crystal 4H-SiC heat spreaders. The superior surface quality of the SiC substrates allows for high-quality bonding and results in low thermal resistance at semiconductor / heat spreader interface. As mentioned, CVD diamond has also been employed as a heat spreader in both VECSELs and MECSELs due to the higher thermal conductivity [21]–[23]. However, the higher price as well as the lower surface quality hinder its full implementation. In this regard, larger-size single-crystal SiC wafers are available (currently up to 150-mm diameter) and at lower costs, enabling wafer-scale gain chip manufacturing.

Bonding of the gain membrane to the first SiC substrate is realized by using a low-temperature plasma-assisted process, followed by NH_4OH-based removal of the GaAs growth

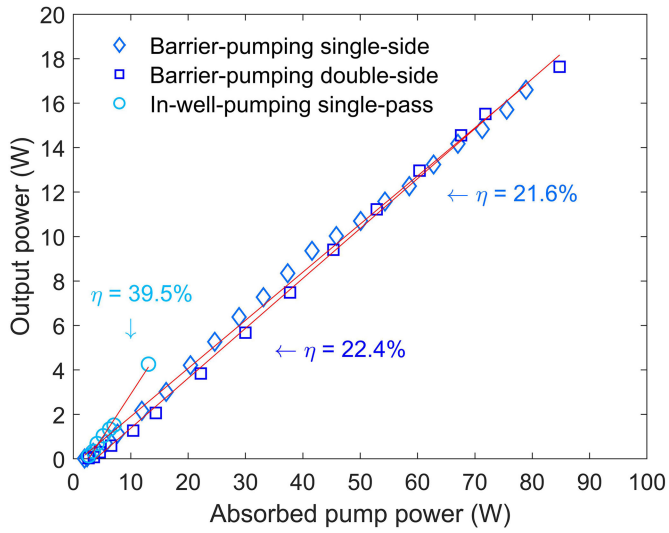

Fig. 2. Output powers vs. absorbed pump powers for the MECSEL under various pumping conditions including barrier-pumping single-side, barrier-pumping double-side, and in-well-pumping single-pass configuration. η represents the slope efficiencies of the curves.

substrate and a HF-based etch of a high-Al-content AlGaAs etch stop layer. The SiC/epi stack is then bonded to a second SiC substrate to form a dual-heat spreader structure [12]. Plasma-enhanced chemical vapor deposition was then used to deposit single layer SiO_2 anti-reflection (AR) coatings, centered at 1070 nm, onto the external faces of the SiC. Fig. 1(b) shows a schematic of the completed gain chip which is clamped between two water-cooled copper mounts connected to a chiller kept at 10 °C. Thin indium foil (blue lines) is placed on both sides of the MECSEL to improve thermal contact with the copper mounts.

Our MECSEL test setup consists of a linear standing-wave cavity formed by two 1% output couplers with radius of curvature of 250 mm and 150 mm, with a cavity length of 350 mm. The gain chip is optically pumped with a fiber-coupled 808 nm diode laser for barrier pumping experiments, and with a 1070 nm fiber laser for in-well pumping. In both experiments, to enable mode matching, the laser mode radius at the gain chip was calculated to be 190 μm, and the pump beam radius was set at 200 μm. Double-side barrier pumping of the gain medium was also investigated as a comparison. In this case, an additional identical 808 nm diode laser was used to simultaneously pump the back of the gain chip. The total output power reported was collected simultaneously from both output couplers.

III. Barrier-Pumping VS. in-Well Pumping

Fig. 2 shows the resulting CW output powers as a function of the absorbed pump power for barrier-pumped and in-well pumped MECSELs. The slope efficiencies and output powers of the single and double-side barrier-pumped experiments are almost the same with values of 21.6% / 22.4% and 16.6 W / 17.6 W respectively. The maximum output powers were reached at an absorbed pump power of 80 W and 85 W respectively, and laser threshold was achieved at 2.5 W. Thermal roll-over was observed for higher pump powers. It is noted that ~95% of the incident 808 nm laser power is absorbed with negligible reflected power due to the AR coating.

One of the options to further increase the power scaling in these devices is to operate the laser at a lower pump intensity to reduce the transparency density [18]. This, however, is not very practical in semiconductor lasers as it would require a reduction in the QW number which in turn would reduce the total gain. As a consequence, lower cavity losses would be required. Such requirements are further hampered by the use of intracavity heat spreader such as SiC and diamond which add additional losses to the resonator. Therefore, the most efficient solution to reduce the heat generation and delay the thermal roll-over would be to pump the QW with pump photon energies close to the laser photon energy, thus lowering the quantum defect defined as $\delta_q = 1 - \lambda_{pump}/\lambda_{laser}$. For a laser designed to operate at 1178 nm and using an excitation wavelength of 808 nm (barrier-pumping), δ_q is 31.4%. On the other hand, using an excitation wavelength of 1070 nm, δ_q reduces to 9.2% which is about three times smaller.

The corresponding in-well pumped sample was tested under the same conditions (T = 10 °C), output coupling (total of 2%), and mode size (~200 μm). Considering only the change in pump wavelength, an improvement in the slope efficieny of a factor 1070 nm/808 nm = 1.32 would be expected, yielding an expected in-well pumped slope efficiency of ~29%. However, our experiment yields a slope efficiency of 39.5%. We hypothesize that this improvement is due to the better beam quality of the in-well-pumped laser (1070 nm fiber laser) compared to the barrier-pumped laser (808 nm diode laser). It is well known that the beam quality of a multi-mode fiber-coupled diode laser is substantially worse than that of a single-model fiber laser ($M^2 < 1.05$) [24]. Therefore, we adjusted the mode size and pump focus to account for the different optimal mode size ratio.

While the threshold is comparable to the barrier-pumped samples, the slope efficiency is significantly higher compared to our previously barrier-pumped MECSELs at a similar heatsink temperature of 10 °C [14]. For a single pass of the pump laser through the active region, the absorbed power is approximately 9.5% of the incident pump power, therefore limiting the maximum output power. The slight undulation of the output power for the barrier-pumping single side experiment is thought to be caused by mode/polarization hopping. Moreover, it is important to note that no thermal roll-over was observed and the output power was only limited by the available input power.

IV. Multi-Pass for in-Well Pumping

To obtain a decent gain per pass, a relatively large carrier density is required, which unfortunately reduces the absorption in the quantum well. The transparency density also moves to higher energies, and shorter wavelengths are required for a reasonable absorption, therefore causing the minimum quantum defect to increase. An increase of the number of passes through the gain medium is thus necessary to achieve high absorbed powers while mantaining a low quantum defect.

In solid-state disk laser the number of pump passes has been increased over the years which has allowed for a reduction in the thickness of the disk and hence their heat loads and transparency

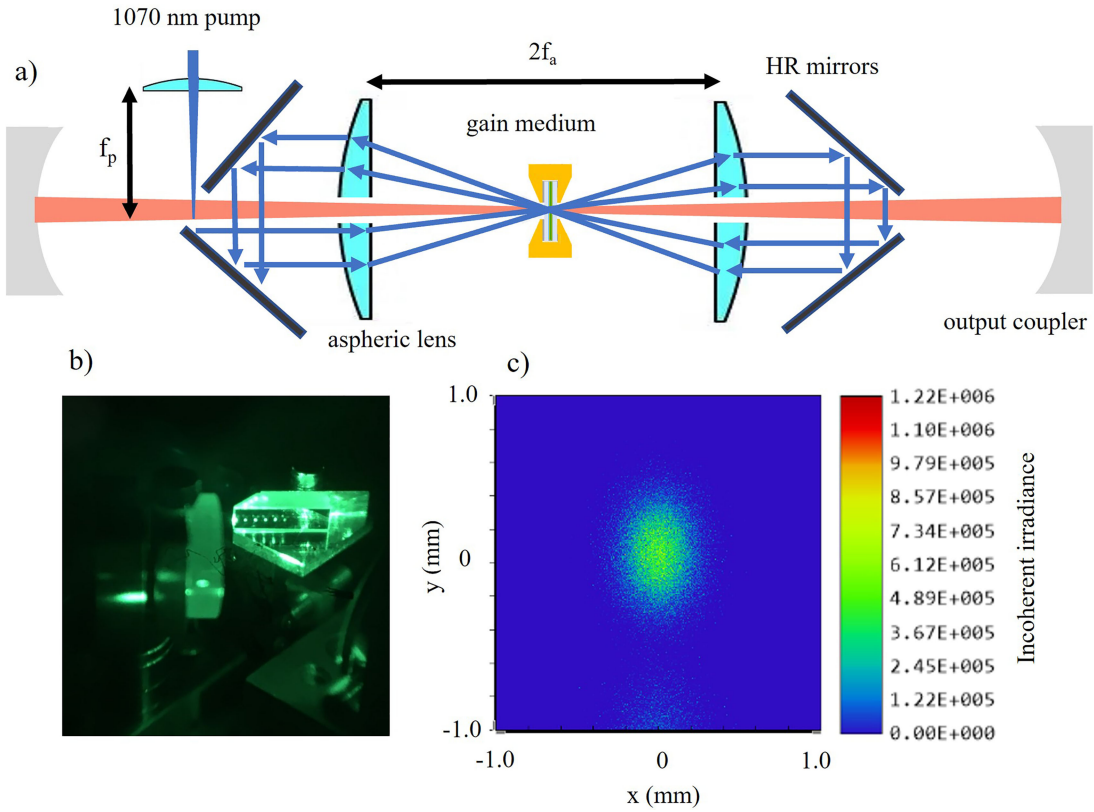

Fig. 3. (a) Schematic of our multi-pass in-well pumping setup. The pump laser is focused to a diameter of 3 mm before being reflected by the mirror and the aspheric lenses collimate the beam onto the sample. The beam is shifted following each roundtrip by the last mirror. (b) Image taken with an IR viewer of the shifted mirror showing multiple passes. (c) Zemax simulation of the 2D pump beam profile at the gain chip with 8 passes.

density, therefore achieving high output powers [25], [26]. It is noted that one could use the standard multi-pass pumping setup employed for such solid-state disk lasers where a parabolic mirror focuses the pump laser onto the gain medium and subsequently re-collimates the transmitted light [27], resulting in many passes with only few optical elements. However, such commercial systems are designed for larger spot sizes and are typically optimized for different wavelengths.

In this work, we designed, modeled, and implemented a 4f multi-pass pump-laser circulator in transmission geometry as depicted in Fig. 3(a). The setup consists of two pairs of flat high-reflectivity mirrors at 1070 nm with each pair forming a retroreflector set. The mirror axes are displaced with respect to each other to introduce a small lateral shift of the pump beam (by $\sim$2 mm) upon each retroreflection. A pair of aspheric lenses ($f_a = 5$ cm, D = 2.54 cm; Thorlabs Inc.), positioned in a confocal geometry, route the incident pump beam through the focus twice in each rountrip. The on-axis distance of the mirror pairs to the aspheric lenses are also f_a, thus forming a 4f circulator. The pump laser, directed through a small opening on one of the mirrors, is focused using a lens with $f_p = 20$ cm to a spot size of 7.5 μm at a distance of f_a away from the first aspheric lens. The beam is then collimated by the first aspheric lens to a spot size of 250 μm on the gain chip (placed at the focal distance of the lens). The transmitted light is then shifted by the second mirror pair and re-collimated by the second lens to the gain chip. This process repeats for many rountrips until the pump beam exits when its position becomes larger than the radius of the lens. Fig. 3(b) shows an IR image of the passes being reflected at the surface of the shifted mirror.

The MECSEL cavity is completed by two external dielectric mirrors (output couplers) with total transmissivity of 2%. The cavity mode is directed through holes with 3 mm diameter drilled in the center of each aspheric lens. A good overlap between the pump beam and the laser mode is necessary to attain low losses and therefore low threshold and subsequent high output power. Fig. 3(c) shows the simulated ray-tracing (Zemax) 2D beam profile at the gain medium with 8 circulating passes indicating the feseability of achieving a good multi-pass overlap and subsequent mode-matching. The ellipticity seen in the beam profile is due to the imperfect overlap or residual aberrations in the lenses.

Fig. 4 shows the output power versus the absorbed pump power of the in-well pumped MECSEL at 10 °C with 8 pump passes. 55% of the input power was measured to be absorbed with 8 passes. The output power of 28.5 W at an absorbed pump power of 120 W constitutes a record for MECSELs in general as well as for in-well pumping of any SDLs. As expected by the lower quantum defect, the slope efficiency of 28% is higher than the barrier-pumping experiment, therefore confirming the reduced heat generation in the active region. Similar to Fig. 2, the slight modulation of the output power may be due to mode/polarization hopping and will be investigated in future efforts.

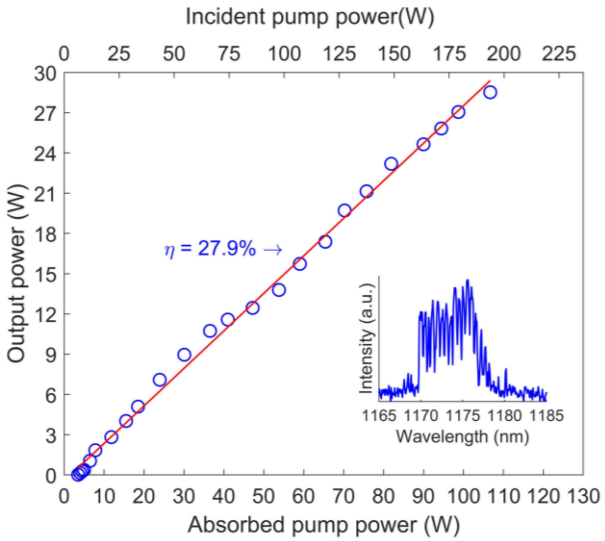

Fig. 4. Power output vs. absorbed pump power of the multi-pass in-well pumped MECSEL showing a maximum output power of 28.5 W with no evidence of thermal roll-over. The inset depicts the multi-mode spectrum at an input power of 135 W.

A higher number of passes can be achieved by reducing the gap between the two flat mirrors where the input laser focuses. However, this is limited by the size of the lasing mode, which also passes through the gap between the pump mirrors. Moreover, the size of the aspheric lenses plays a role since the pump laser shifts outwards every roundtrip. Different cavity configurations and aspheric lens sizes are the focus of follow-on work.

The slope efficiency of the multi-pass experiment is, however, lower than that recorded in the single-pass (39.5%) in-well pumping setup. The reduced slope efficiency of the multi-pass experiment compared to the single pass is thought to be caused by the imperfect overlap between the multiple pump laser passes and laser mode.

The inset in Fig. 4 shows the multimode spectrum recorded at an absorbed pump power of 75 W. At such high input power, the full-width-at-half-maximum (FWHM) was measured to be ∼8 nm centered at 1174 nm.

Finally, this wavelength range is particularly interesting for sodium guide star applications thanks to the OPSLs capability of frequency converting the fundamental signal via non-linear crystals. Narrow linewidth around 589 nm is required to excite the D_{2a} sodium transition line, therefore necessitating additional intracavity optics to reduce the FWHM.

V. Wavelength Tunability: Guidestar Application

In the development of sodium guide star lasers, VECSELs have attracted attention due to their simplicity and low cost, while still allowing for high power operation with good beam quality. Recent works of note include the demonstration of 19 W at 1178 nm operating in single mode [28], and other yellow demonstrations which include a 20 W output power measured employing a V-shape cavity with an intra-cavity frequency-doubling LBO crystal [29]–[31]. Recently we reported the first MECSEL operating at 1178 nm in a barrier-pumping configuration [14].

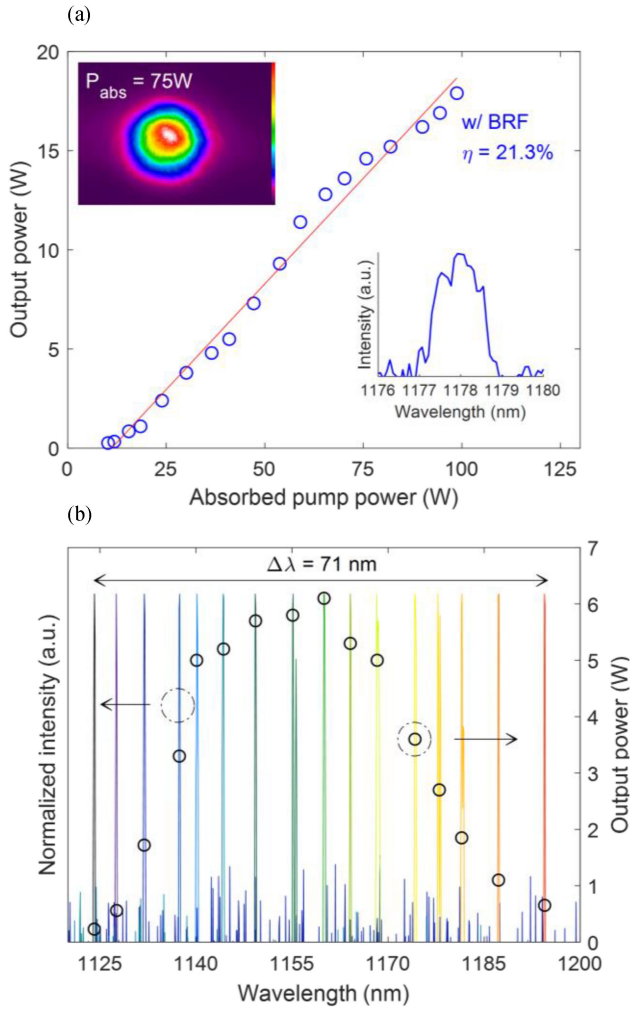

Fig. 5. (a) Output power vs. absorbed power of the multi-pass in-well pumped MECSEL using a 2-mm-thick BRF. The insets show the spectrum tuned at 1178 nm with a linewidth of 1.7 nm and the beam profile of the laser output taken at 75 W of absorbed pump power. (b) Normalized emission spectra using a 2-mm-thick BRF. The output power was recorded under 40 W of absorbed pump power at a heatsink temperature of 10 °C.

To fix the lasing wavelength at 1178 nm as required for sodium guide star applications (for further frequency conversion to 589 nm), a 2 mm birefringent filter (BRF) is placed inside the cavity for tuning to the target wavelength. Fig. 5(a) shows the output power at $\lambda = 1178$ nm as a function of the absorbed pump power. A slightly lower slope efficiency of 19.4% was measured compared to the experiment without the BRF mainly due to the additional losses introduced by the intracavity element. A maximum output power of 18 W at an absorbed pump power of 110 W was measured. This represents an improvement of more than 5 W with respect to our barrier-pumped results [14]. The bottom-right inset in Fig. 5(a) depicts the spectrum measured with the BRF. We obtained a narrower linewidth of 1.7 nm compared to the multimode FWHM of the experiment without the BRF. Multiple modes can be seen at longer and shorter wavelengths which are caused by the etalon effect of the SiC heat spreaders. The measured wavelength separation is close to the FSR ≈ 0.3 nm from the subcavity formed by the two ∼500 μm thick SiC substrates. Since the AR coatings on the SiC

substrates were designed for the pump wavelength, this results in a low-finesse etalon at the emission wavelength. The beam profile of the 1178 nm MECSEL using the BRF taken at an absorbed pump power of 75 W is shown in the top-left inset, exhibiting a good quality Gaussian beam for such high input power.

Due to the broad gain bandwidth of semiconductor materials, wavelength tunability up to 172 nm employing external-cavity diode lasers have been demonstrated [32]. However, typical quantum wells OPSLs near 1 μm have shown limited wavelength tunability [33], [34]. As described in reference [10], MECSELs exhibit an increased tuning range, realized via the use of broadband dielectric mirrors and due to the position of the resonant periodic gain away from the global cavity nodes.

We achieved a tunability of 71 nm as shown in Fig. 5(b). This range is very similar to our previous report of 75 nm obtained with a barrier-pumping scheme with an 11 QW sample [14], nearly limited by the FSR of the BRF which is 82 nm. The wavelength-dependent output power shown on the right y-axis of Fig. 5(b) was recorded at an absorbed pump power of 40 W. The maximum power of 6 W was measured at a wavelength of 1160 nm which partially explains the higher threshold of Fig. 5(b) compared to Fig. 4. In fact, at low temperature (pump power) the wavelength of the gain peak in our samples is significantly shorter than 1178 nm, as they were designed for high-power operation at that wavelength.

VI. Conclusion

In summary, we studied the output power enhancement for in-well pumping of a MECSEL compared to the more standard barrier-pumping technique. A 20-QW resonant-periodic-gain membrane was specifically designed and synthesized to increase the absorbed pump power. Despite the large number of QWs, the sample did not show any sign of degradation due to strain and exhibited surface quality sufficient for direct bonding, hence indicating the feasibility of growing many QWs for enhanced pump absorption in a MECSEL. For a single pump pass, the slope efficiency for in-well pumping increased to 39.5% compared to 21.6% for barrier pumping. A record output power for the MECSEL (as well as for any in-well pumped VECSEL) of 28.5 W was demonstrated by adopting a 4f multi-pass pumping architecture. A 2-mm-thick BRF was used to tune the emission wavelength to 1178 nm and 18 W of output power was measured with a FWHM of 1.7 nm. Additionally, the laser wavelength was tuned over a range of 71 nm, from 1124 nm to 1195 nm using 2% output coupling in the external laser cavity. These results demonstrate the feasibility of employing MECSELs in future compact and low-cost sodium guide star lasers.

References

[1] M. Kuznetsov, F. Hakimi, R. Sprague, and A. Mooradian, "Semiconductor lasers with circular TEM beams," *IEEE Photon. Technol. Lett.*, vol. 9, no. 8, pp. 1063–1065, Aug. 1997.

[2] P. Holl *et al.*, "Recent advances in power scaling of gasb-based semiconductor disk lasers," *IEEE J. Sel. Topics Quantum Electron.*, vol. 21, no. 6, pp. 324–335, Nov./Dec. 2015.

[3] O. G. Okhotnikov, Ed. *Semiconductor Disk Lasers: Physics and Technology*. Hoboken, NJ, USA: Wiley, 2010.

[4] M. Guina, A. Rantamäki, and A. Härkönen, "Optically pumped VECSELs: Review of technology and progress," *J. Phys. D. Appl. Phys.*, vol. 50, no. 38, 2017, Art. no. 383001.

[5] B. Rudin *et al.*, "Highly efficient optically pumped vertical-emitting semiconductor laser with more than 20 W average output power in a fundamental transverse mode," *Opt. Lett.*, vol. 33, no. 22, pp. 2719–2721, 2008.

[6] Z. Yang, A. R. Albrecht, J. G. Cederberg, and M. Sheik-Bahae, "Optically pumped DBR-free semiconductor disk lasers," *Opt. Exp.*, vol. 23, no. 26, 2015, Art. no. 33164.

[7] H. Kahle *et al.*, "Semicond. membrane external-cavity Surf.-Emitting laser (MECSEL)," *Optica*, vol. 3, no. 12, pp. 1506–1512, 2016.

[8] H. Kahle *et al.*, "Comparison of single-side and double-side pumping of membrane external-cavity surface-emitting lasers," *Opt. Lett.*, vol. 44, no. 5, pp. 1146–1149, 2019.

[9] H.-M. Phung *et al.*, "Power scaling and thermal lensing in 825 nm emitting membrane external-cavity surface-emitting lasers," *Opt. Lett.*, vol. 45, no. 2, p. 547, 2020.

[10] Z. Yang, A. R. Albrecht, J. G. Cederberg, and M. Sheik-Bahae, "80 nm tunable DBR-free semiconductor disk laser," *Appl. Phys. Lett.*, vol. 109, no. 2, 2016, Art. no. 022101.

[11] S. Mirkhanov *et al.*, "DBR-free semiconductor disc laser on SiC heat-spreader emitting 10.1 W at 1007 nm," *Electron. Lett.*, vol. 53, no. 23, pp. 1537–1539, 2017.

[12] Z. Yang *et al.*, "16 W DBR-free membrane semiconductor disk laser with dual-SiC heatspreader," *Electron. Lett.*, vol. 54, no. 7, pp. 430–432, 2018.

[13] A. Broda, B. Jeżewski, M. Szymański, and J. Muszalski, "High-power 1770 nm emission of a membrane external-cavity surface-emitting laser," *IEEE J. Quantum Electron.*, vol. 57, no. 1, pp. 1–6 2021.

[14] D. Priante *et al.*, "Demonstration of a 20 W membrane-external-cavity surface-emitting laser for sodium guide star applications," *Electron. Lett.*, vol. 57, p. 337, 2021.

[15] S.-S. Beyertt, *et al.*, "Efficient gallium–arsenide disk laser," *IEEE J. Quantum Electron.*, vol. 43, no. 10, pp. 869–875, Oct. 2007.

[16] C. M. N. Mateo *et al.*, "Enhanced efficiency of AlGaInP disk laser by in-well pumping," *Opt. Exp.*, vol. 23, no. 3, 2015, Art. no. 2472.

[17] C. M. Mateo *et al.*, "Efficiency and power scaling of in-well and multi-pass pumped AlGaInP VECSELs," *Vert. Extern. Cavity Surf. Emit. Lasers VI*, vol. 9734, Mar. 2016, Art. no. 973410.

[18] U. Brauch *et al.*, "Schemes for efficient QW pumping of AlGaInP disk lasers," *Vert. Extern. Cavity Surf. Emit. Lasers VII*, vol. 10087, Feb. 2017, Art. no. 1008703.

[19] C. M. N. Mateo *et al.*, "2.5 W continuous wave output at 665 nm from a multi-pass and quantum-well-pumped AlGaInP vertical-external-cavity surface-emitting laser," *Opt. Lett.*, vol. 41, no. 6, pp. 1245–1248, 2016.

[20] S. W. Corzine, R. S. Geels, J. W. Scott, R. H. Yan, and L. A. Coldren, "Design of fabry-perot surface-emitting lasers with a periodic gain structure," *IEEE J. Quantum Electron.*, vol. 25, no. 6, pp. 1513–1524, Jun. 1989.

[21] R. G. Bedford *et al.*, "Power-limiting mechanisms in VECSELs." in *Enabling Photonics Technologies For Defense, Security, and Aerospace Applications*. vol. 5814, Bellingham, Washington USA: International Society for Optics and Photonics, 2005.

[22] R. Wei *et al.*, "Thermal conductivity of 4H-SiC single crystals," *J. Appl. Phys.*, vol. 113, no. 5, 2013, Art. no. 053503.

[23] G. A. Slack, "Thermal conductivity of pure and impure silicon, silicon carbide, and diamond," *J. Appl. Phys.*, vol. 35, no. 12, pp. 3460–3466, 1964.

[24] A. Laurain, J. Hader, and J. V. Moloney, "Modeling and optimization of transverse modes in vertical-external-cavity surface-emitting lasers," *J. Opt. Soc. Am. B*, vol. 36, no. 4, pp. 847–854, 2019.

[25] K. Schuhmann *et al.*, "Thin-disk laser pump schemes for large number of passes and moderate pump source quality," *Appl. Opt.*, vol. 54, no. 32, 2015, Art. no. 9400.

[26] Erhard, S., M. Karszewski, Chr Stewen, A. Giesen, K. Contag, and A. Voss "Pumping schemes for multi-kW thin disk lasers," in *Adv. Solid State Lasers*, vol. 34, 2014, Paper MB16.

[27] A. Voss *et al.*, "Thin-disk laser operation of pr 3 +, mg 2 + : Sral 12 o 19," *Opt. Lett.*, vol. 39, no. 5, pp. 1322–1325, 2014.

[28] E. Kantola, J.-P. Penttinen, S. Ranta, and M. Guina, "72-W vertical-external-cavity surface-emitting laser with 1180-nm emission for laser guide star adaptive optics," *Electron. Lett.*, vol. 54, no. 19, pp. 1135–1137, 2018.

[29] S. E. Rako *et al.*, "High-power single-frequency intracavity doubled VECSEL at 589 nm for sodium guidestar," *Vertical External Cavity Surface Emitting Lasers (VECSELs) X*. vol. 11263. Bellingham, Washington USA: International Society for Optics and Photonics, 2020.

[30] M. Fallahi *et al.*, "5-W yellow laser by intracavity frequency doubling of high-power vertical-external-cavity surface-emitting laser," *IEEE Photon. Technol. Lett.*, vol. 20, no. 20, pp. 1700–1702, Oct. 2008.
[31] E. Kantola, T. Leinonen, S. Ranta, M. Tavast, and M. Guina, "High-efficiency 20 W yellow VECSEL," *Opt. Exp.*, vol. 22, no. 6, 2014, Art. no. 6372.
[32] E. L. Eng, D. G. Mehuys, M. Mittelstein, and A. Yariv, "Broadband tuning (170 nm) of InGaAs quantum well lasers," *Electron. Lett.*, vol. 26, no. 20, pp. 1675–1677, 1990.
[33] L. Fan *et al.*, "Tunable high-power high-brightness linearly polarized vertical-external-cavity surface-emitting lasers," *Appl. Phys. Lett.*, vol. 88, no. 2, pp. 1–3, 2006.
[34] L. Fan *et al.*, "Extended tunability in a two-chip VECSEL," *IEEE Photon. Technol. Lett.*, vol. 19, no. 8, pp. 544–546, Apr. 2007.

Davide Priante received the B.S. degree in material science and engineering from Padova University, Italy, in 2013 and the M.S. degree in electrical engineering from the King Abdullah University of Science and Technology (KAUST) in 2015. He completed the Ph.D. degree from KAUST in 2019 with a research focus on the fabrication and characterization of large-bandgap group III-Nitride semiconductor optoelectronic devices. He is currently a Postdoctoral Fellow with the University of New Mexico (UNM), Albuquerque, USA. His research includes the design and characterization of GaAs membrane external-cavity surface-emitting lasers.

Mingyang Zhang received the B.S. degree in optical information of science and technology from Guizhou University, Guiyang, China, in 2015, and the M.S. degree with distinction in optics and photonics from Imperial College London, London, the U.K., in 2016. He is currently working toward the Ph.D. degree in optical science and engineering with the University of New Mexico, Albuquerque, the U.S. From 2016 to 2017, he was an Optical Engineering with Han's Laser Technology Co., Ltd., Shenzhen, China. From 2017 to 2018, he was a Laser Engineer with Tsinghua University, Beijing, China. Since 2018, he has been a Ph.D. Student with the Physics Department, the University of New Mexico, Albuquerque. His research interest includes ultrafast science, extreme nonlinear optics and laser technology.

Alexander R. Albrecht received the M.S. and Ph.D. degrees in physics from the University of New Mexico, Albuquerque, in 2009 and 2001, respectively. From 2009 to 2014, he was a Postdoctoral Researcher with the Center for High Technology Materials and Department of Physics and Astronomy, University of New Mexico. Since 2014, he has been a Research Assistant Professor with the Department of Physics and Astronomy, University of New Mexico. His research interests include the development of high-power semiconductor vertical external-cavity surface-emitting lasers based on quantum well and quantum dot active regions, and optical refrigeration and radiation-balanced lasers in rare-earth-doped systems.

Roman Bek received the B.S. degree in physics from the University of Konstanz, Konstanz, Germany, in 2010, the M.S. and Ph.D. degrees in physics from the University of Stuttgart, Stuttgart, Germany, in 2012 and 2018, respectively. From 2017 to 2018, he was an Assistant Lecturer with Stuttgart University of Applied Sciences. In 2019, he founded Twenty-One Semiconductors GmbH, Neckartenzlingen, Germany to commercialize novel semiconductor membrane laser gain chips for biomedical and spectroscopic applications. He is currently the CTO of Twenty-One Semiconductors GmbH. His research interests include III-V semiconductor epitaxy and surface-emitting semiconductor lasers.

Michael Zimmer received the B.S. and M.S. degrees in physics in 2015 and 2018, respectively, from the University of Stuttgart, Stuttgart, Germany, where he is currently working toward the Ph.D. degree with the Institute of Semiconductor Optics and Functional Interfaces.

Since 2019, he has been a Laser Engineer with Twenty-One Semiconductors GmbH, Neckartenzlingen, Germany. His research interests include vertical-cavity surface-emitting laser, electrically pumped VECSEL and quantum dot-based lasers.

Catherine L. Nguyen was born in Phc Long, Vietnam, in 1975 and attended Coastline Community College in Fountain Valley, CA.

She has 20 years of experience in semiconductor processing, holding positions with Touchdown Technologies, Exponent Photonics, Global Communication Semiconductors, Soraa Laser Diode (now KYOCERA SLD Laser), and Crystalline Mirror Solutions (CMS). Following the acquisition of CMS by Thorlabs, she is currently a Process Engineer with Thorlabs Crystalline Solutions, in Santa Barbara, CA.

Ms. Nguyen has extensive microfabrication expertise in compound semiconductor materials, spanning photolithography, thin film deposition, polishing, direct bonding, reactive-ion and wet-chemical etching, as well as electroplating processes.

David P. Follman was born in Manchester, CT in 1974. He received the B.S. degree in materials science and engineering from Brown University, Providence, R.I., in 1997, and the M.S. degree in materials from the University of California, Santa Barbara, in 2004.

From 2008 to 2014, he was a Lead Process Engineer with FLIR Electro-Optical Components (formerly Aerius Photonics, LLC). In 2014, he joined Crystalline Mirror Solutions (CMS) as Senior Development Engineer and then in 2016 was promoted to Global Production Manager. CMS was acquired by Thorlabs Inc. in December 2019, and Mr. Follman is currently Principal Manufacturing Engineer III for Thorlabs Advanced Photonics. He holds three patents and has published more than 29 journal articles.

Mr. Follman was the Recipient of the National Science Foundation GK12 Fellowship.

Garrett D. Cole was born in San Jose, CA, in 1979. He received the B.S. degree in materials engineering from the California Polytechnic State University, San Luis Obispo, in 2001 and the Ph.D. degree in electronic materials from the University of California, Santa Barbara, in 2005.

From 2005 to 2006, he was a Research Scientist with Aerius Photonics LLC (now FLIR Electro-Optical Components) and from 2006 to 2008, he held a postdoctoral position with Lawrence Livermore National Laboratory. In 2008, he moved to Vienna and was a Marie Curie Fellow of the Austrian Academy of Sciences, transitioning to a Universitätsassistent in the Faculty of Physics with the University of Vienna in 2011. In 2014, he founded Crystalline Mirror Solutions (CMS) to commercialize substrate-transferred single-crystal coatings for laser-based metrology and manufacturing systems. CMS was acquired by Thorlabs Inc. in December 2019, and Dr. Cole is currently the Technology Manager of Thorlabs Crystalline Solutions in Santa Barbara, CA. He holds nine patents, has authored two book chapters, and has authored or coauthored more than 50 journal articles. His research interests include advanced micro- and nanofabrication techniques, cavity optomechanics, compound semiconductor materials, precision measurement, as well as surface-emitting laser and amplifier systems.

Dr. Cole's awards and honors include the LIGHT2015 Young Photonics Entrepreneur Award, the Berthold Leibinger Innovationspreis, and an SPIE Prism Award.

Mansoor Sheik-Bahae (Member, IEEE) received the B.S. degree in electrical engineering from Catholic University, Washington, DC, in 1980, and the Ph.D. degree in electro-physics from the State University of New York at Buffalo, SUNY-Buffalo, in 1987. He is a Distinguished Professor with the Department of Physics and Astronomy, the University of New Mexico (UNM), Albuquerque, NM (USA). He spent seven years with CREOL (University of Central Florida) before joining UNM in 1994. He was elected an OSA Fellow (2000), and was the Co-Recipient of the OSA's Wood Prize (2012).